A c-di-GMP-Based Switch Controls Local Heterogeneity of Extracellular Matrix Synthesis which Is Crucial for Integrity and Morphogenesis of *Escherichia coli* Macrocolony Biofilms

Diego O. Serra and Regine Hengge

Institut für Biologie/Mikrobiologie, *Humboldt-Universität zu Berlin, 10115 Berlin, Germany*

Correspondence to Regine Hengge: *Institut für Biologie/Mikrobiologie, Humboldt-Universität zu Berlin, Philippstr. 13—Haus 22, 10115 Berlin, Germany. regine.hengge@hu-berlin.de*
https://doi.org/10.1016/j.jmb.2019.04.001
Edited by Kirsten Jung

Abstract

The extracellular matrix in macrocolony biofilms of *Escherichia coli* is arranged in a complex large-scale architecture, with homogenic matrix production close to the surface, whereas zones further below display pronounced local heterogeneity of matrix production, which results in distinct three-dimensional architectural structures. Combining genetics, cryosectioning and fluorescence microscopy of macrocolony biofilms, we demonstrate here *in situ* that this local matrix heterogeneity is generated by a c-di-GMP-dependent molecular switch characterized by several nested positive and negative feedback loops. In this switch, the trigger phosphodiesterase PdeR is the key component for establishing local heterogeneity in the activation of the transcription factor MlrA, which in turn activates expression of the major matrix regulator CsgD. Upon its release of direct inhibition by PdeR, the second switch component, the diguanylate cyclase DgcM, activates MlrA by direct interaction. Antagonistically acting PdeH and DgcE provide for a PdeR-sensed c-di-GMP input into this switch and—via their spatially differentially controlled expression—generate the long-range vertical asymmetry of the matrix architecture. Using flow cytometry, we show heterogeneity of CsgD expression to also occur in spatially unstructured planktonic cultures, where it is controlled by the same c-di-GMP circuitry as in macrocolony biofilms. Quantification by flow cytometry also showed $CsgD^{ON}$ subpopulations with distinct CsgD expression levels and revealed an additional fine-tuning feedback within the PdeR/DgcM-mediated switch that depends on c-di-GMP synthesis by DgcM. Finally, local heterogeneity of matrix production was found to be crucial for the tissue-like elasticity that allows for large-scale wrinkling and folding of macrocolony biofilms.

Introduction

Even in homogeneous environments such as well-mixed liquid media, some cells in a clonal population can show gene expression patterns that are different from those of their siblings. Often, this manifests as a bifurcation of the population into subpopulations with distinct phenotypes, a phenomenon referred to as bistability [1,2]. Such diversification is usually interpreted as a bet-hedging strategy that allows bacteria to persist in fluctuating enviroments [3] or in terms of a division of labor in a microbial community that promotes general fitness or generates emergent properties that each subpopulation on its own would not have been able to generate [4,5]. Bistability can be brought about by regulatory switches involving positive or double-negative feedback loops that amplify stochastic fluctuations (i.e., noise) in the levels or activities of regulatory components [2,3,6].

Phenotypic heterogeneity has been observed in bacterial biofilms, that is, large structured bacterial communities usually growing on surfaces [7–9]. Within biofilms, bacteria show high resistance against adverse conditions, including antibiotic treatments. As a consequence, biofilms are commonly associated with chronic, difficult-to-treat infections, constituting a serious public health problem [8,10,11]. Biofilms are protected and hold together by a self-produced extracellular matrix typically composed of exopolysaccharides, amyloid fibers, secreted proteins and

extracellular DNA [9]. In macrocolony biofilms grown over several days on semi-solid agar plates, the extracellular matrix also confers elasticity, that is, mechanical properties that enable the biofilm as a whole to fold into complex morphological patterns such as wrinkles or ridges [12–14]. In macrocolony biofilms of many *Escherichia coli* strains, this morphogenesis depends on two major extracellular matrix components with complementary "building material" properties: amyloid curli fibers, which form a cohesive, yet non-elastic network around the cells, and the exopolysaccharide phosphoethanolamine (pEtN)-cellulose which—in particular in a composite with amyloid curli fibers—generates elasticity [12,15,16].

Within macrocolony biofilms of the two model bacteria *E. coli* and *Bacillus subtilis*, matrix production was found to be highly heterogeneous [5,12,17–20]. When analyzed *in situ*, this heterogeneity is actually 2-fold in kind, including both long-range and—in certain biofilm zones—short-range variations, which are caused by different mechanisms. Long-range heterogeneity of matrix production is due to gradients of resources, oxygen and possibly also signaling compounds that build up over long distances by diffusion and bacterial metabolic activities. These gradients have a fundamental impact on genome-wide gene expression patterns [12,15,20,21]. Thus, post-exponentially growing flagellated cells are found in the *E. coli* macrocolony bottom layer (a zone close to the nutrient-containing agar that is only ~15 μm high), whereas the synthesis of curli and pEtN-cellulose occurs in the upper layer (~45 μm high) by cells that are more remote from nutrient sources and therefore enter into stationary phase (see Fig. 1). Matrix-producing cells express the biofilm regulator CsgD, whose own expression depends on RpoS (σ^S), the stationary phase sigma subunit of RNA polymerase, and which positively regulates the synthesis of both curli and pEtN-cellulose [19,20]. Notably, the expression of CsgD and therefore matrix production are not restricted to cells residing in biofilms but also occurs in planktonic cultures during entry into stationary phase [22–24]. Thus, long-range spatial patterns of matrix production within the macrocolony biofilm in general reflect corresponding temporal patterns observable in liquid cultures [20].

However, patterns of matrix production are more complex in structured biofilms. Even within the matrix-

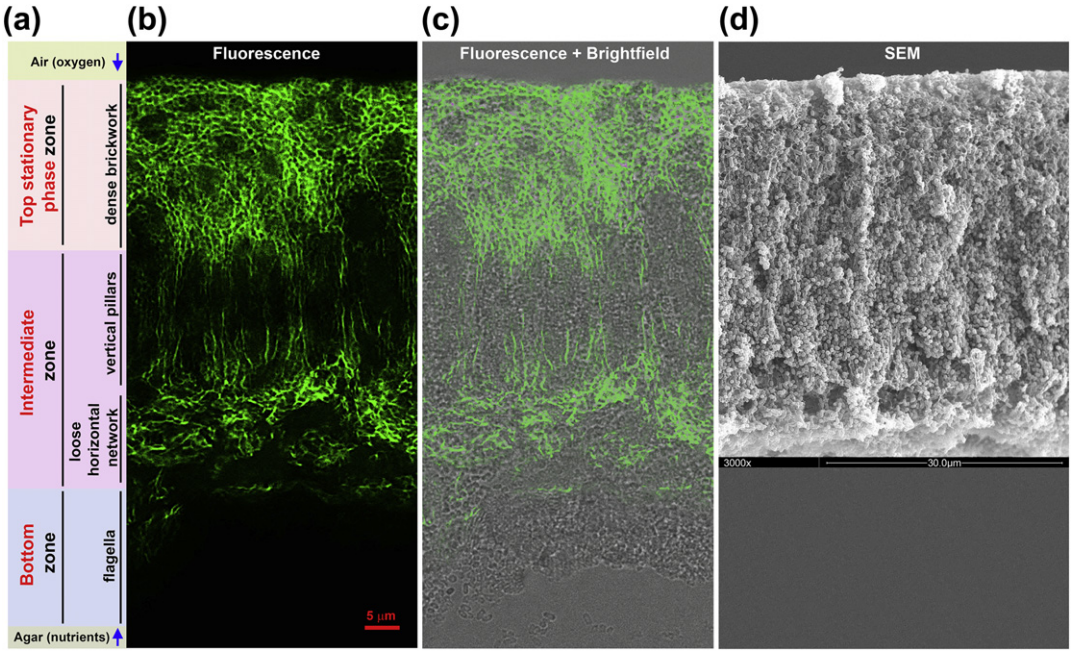

Fig. 1. Vertical stratification of macrocolony biofilms of *E. coli* K-12 strain AR3110. (a) Designation of zones along the vertical axis of a 3-day-old macrocolony biofilm. Fluorescence (b) and (c) merged images of a representative cross section through the AR3110 macrocolony showing the "dense brickwork" of TS-stained curli/pEtN-cellulose composite matrix in the top zone, "vertical pillars" and a "loose horizontal network" mainly of pEtN-cellulose in the intermediate zone as well as a layer of flagellated cells (devoid of fluorescence) in the bottom. The intermediate zone shows pronounced matrix heterogeneity. Especially heterogeneous is the vertical pillar zone where filamentous matrix is interspaced with dark areas that are compactly filled with cells that do not produce matrix (compare panel b with panels c and d). (d) High-resolution SEM image showing a section across the upper layer of an AR3110 macrocolony (the lower layer that is not stabilized by an extracellular matrix, breaks off during preparation for SEM).

generating upper macrocolony layer, an asymmetric organization with architecturally distinct strata was found [20]. In the very top layer, nearly all cells are homogeneously embedded in a curli/pEtN-cellulose matrix, thus generating a dense "brickwork"-like architecture as visualized with the green fluorescent matrix dye thioflavin S (TS; Fig. 1). Further below, the matrix is arranged in "vertical pillars" followed by a "loose horizontal network," which form two sublayers that together represent the intermediate macrocolony zone. In this intermediate zone, patches of matrix-free cells are present right next to the matrix-producing cells that generate these characteristic matrix patterns (Fig. 1). Thus, this pronounced short-range or local heterogeneity of matrix production cannot be a regulatory consequence of locally different external conditions, but is generated endogenously.

Our study presented here addresses the questions of the mechanistic origin of this short-range local heterogeneity within the regulatory network underlying matrix synthesis and its physiological function. The expression of the matrix regulator CsgD is itself tightly regulated, requiring the RpoS-controlled MerR-like transcription factor MlrA, whose activity is in turn crucially controlled by a signaling network mediated by the second messenger bis-(3′-5′)-cyclic dimeric GMP (c-di-GMP) [25,26]. This network involves several c-di-GMP-degrading phosphodiesterases (PDEs) and c-di-GMP-producing diguanylate cyclases (DGCs): PdeR and DgcM, which interact with each other and MlrA, thereby forming a local signaling complex, as well as PdeH and DgcE, which control c-di-GMP input into the PdeR/DgcM module [24,27]. Mathematical modeling has shown that the intricate PdeR/DgcM/MlrA circuitry has the potential to generate bistability [28]. Combining genetic, cryosectioning/microscopic and flow cytometric analyses, we demonstrate here that the endogenous short-range CsgD/matrix heterogeneity in biofilms is indeed generated by the PdeR/DgcM switch module within the *csgD*-controlling c-di-GMP signaling network and that this mechanism even operates in non-spatially structured planktonic cultures. Moreover, our results highlight that local cellular heterogeneity of matrix synthesis is essential for the structural integrity and macroscopic morphogenesis of macrocolony biofilms.

Results

Local heterogeneity of matrix synthesis in *E. coli* macrocolonies is due to the *csgD*-controlling c-di-GMP signaling network with PdeR/DgcM acting as a switching device

The PdeR/DgcM module mediates c-di-GMP input into the activity of MlrA, that is, the intermediate level regulator of the σ^S/MlrA/CsgD transcription factor cascade [22–24]. In particular, PdeR acts as a bifunctional trigger enzyme that inhibits both MlrA and DgcM by direct interaction—as a consequence, *csgD* is not transcribed (see Fig. 2, which summarizes the state of knowledge at the beginning of the present study). During entry into stationary phase, the master PDE PdeH is no longer expressed and its cellular level decreases [20,29,30], while the σ^S-dependent DgcE is induced [20,31] and specifically provides the c-di-GMP that is bound and cleaved by PdeR, thereby "triggering" PdeR to release DgcM and MlrA. This allows the equally bifunctional DgcM to also produce c-di-GMP—thought to provide for a positive feedback in this circuit—and to act as a directly interacting co-activator

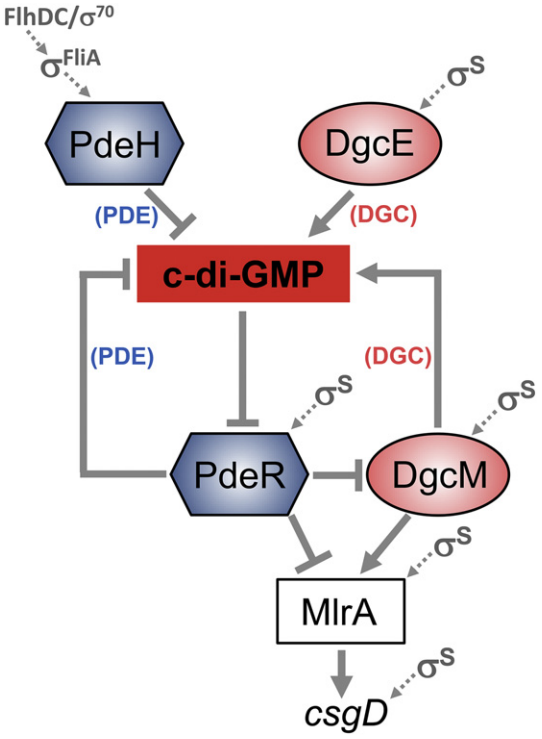

Fig. 2. Model of the c-di-GMP signaling circuitry that controls transcription of *csgD*, encoding the master regulator of biofilm formation. PdeH is the master PDE of *E. coli* whose expression is under the control of the flagellar regulatory cascade. All other components involved depend on σ^S for their expression. PdeR is a "trigger" enzyme that serves as both a PDE and a c-di-GMP-sensing effector. DgcE is a major DGC of *E. coli* with a major impact in the control of CsgD. DgcM is a DGC that specifically serves as directly interacting co-activator for the MerR-like transcription factor MlrA. In still growing cells that experience low c-di-GMP levels due to high activity of PdeH, the "trigger" enzyme PdeR inhibits DgcM and MlrA by direct interaction and, as a consequence, *csgD* is not expressed. When c-di-GMP production by the σ^S-induced DgcE increases, while PdeH is no longer expressed, binding and cleavage of c-di-GMP by PdeR releases DgcM and MlrA, resulting in initiation of *csgD* transcription.

for MlrA at the *csgD* promoter [24,27]. This switch is clearly thrown in nearly all of the starving cells in the "dense brickwork" top layer of a macrocolony, whereas the characteristically heterogeneous patterns of matrix distribution in the intermediate layer could be the result of switching in a subset of cells only.

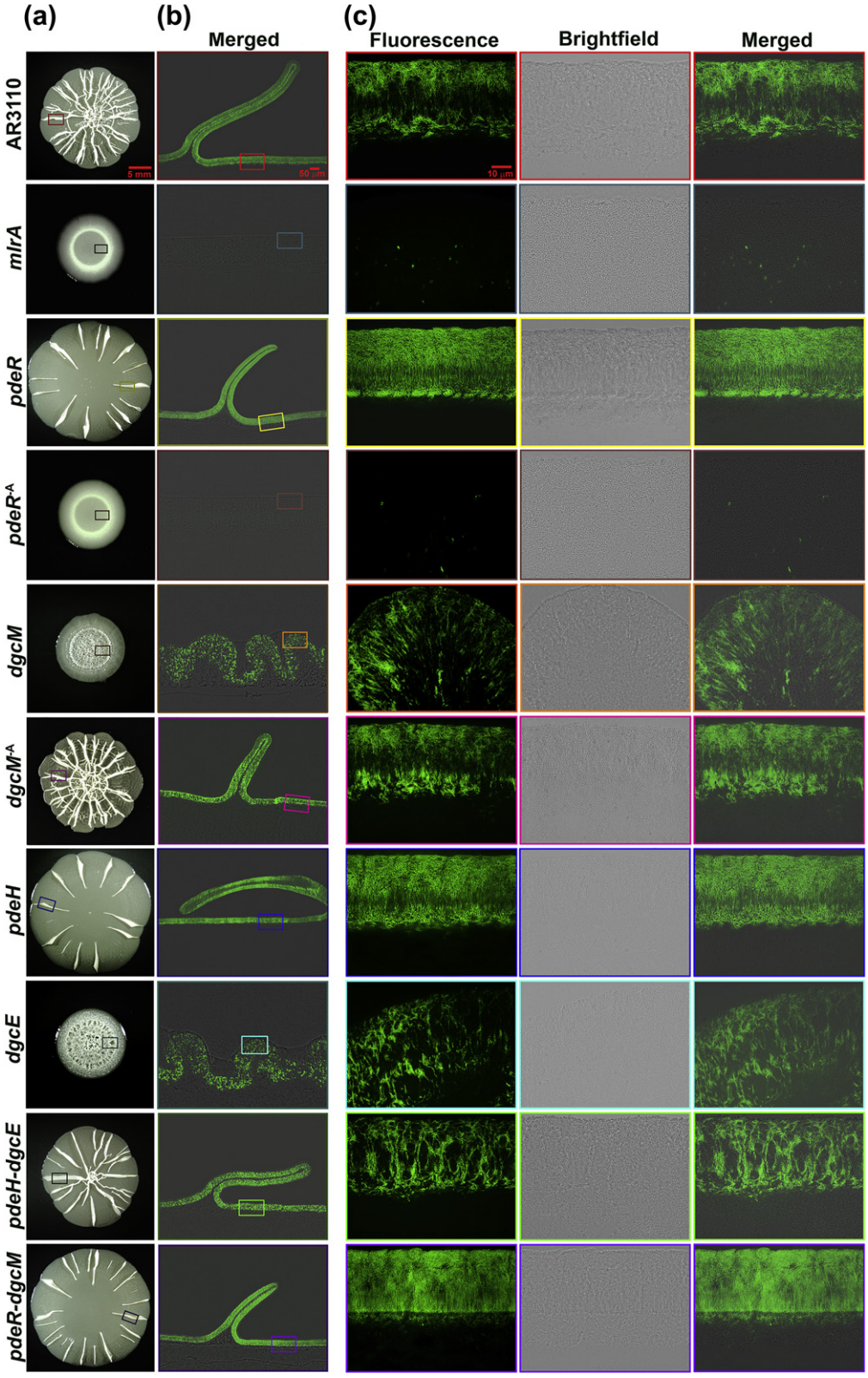

In order to evaluate the role of this c-di-GMP-mediated switch and the contributions of its individual DGCs and PDEs in generating matrix heterogeneity, single and double deletions as well as specific point mutations in these network components were tested for their effects on curli/pEtN-cellulose distribution *in situ* in macrocolonies. All mutations are located in the chromosomal copies of the respective genes to preserve wild-type expression levels and stoichiometries of all factors involved. For a direct comparison of specific mutant behavior, the data with all mutants are combined in Fig. 3, with particularly interesting details of matrix architecture presented at larger magnification and with quantification in Fig. 4.

mlrA

As MlrA is essential for directly initiating *csgD* transcription [32], matrix production remains shut off in the *mlrA* mutant, which results in cryosections essentially devoid of matrix (Fig. 3).

pdeR

As PdeR's inactivation (in its role as an inhibitor of DgcM/MlrA) by c-di-GMP allows DgcM/MlrA to initiate *csgD* transcription, deleting PdeR renders CsgD expression "blind" to the c-di-GMP signal controlled by PdeH/DgcE and eliminates the double-negative feedback loop inherent to the switch module. As a result, DgcM/MlrA is free from inhibition and thus available to initiate *csgD* transcription—provided DgcM and MlrA are expressed, that is, in all cells that contain active σ^S-RNA polymerase [24,27]. Consistent with this scenario, *pdeR* deletion indeed eliminated heterogeneity of matrix synthesis in the intermediate biofilm zone, resulting in a highly homogeneous pattern of vertical pillars and a much denser network of still mostly horizontally arranged matrix below the pillars (Figs. 3c and 4b).

pdeR^{-A}

As shown in liquid cultures, a catalytically inactive PdeR variant (PdeR^{-A}, with the EAL motif changed to AAL) is insensitive to the c-di-GMP signal generated by PdeH/DgcE, therefore behaving as a constitutive "super inhibitor" whose inhibition of MlrA/DgcM cannot be relieved, thus keeping *csgD* expression and matrix production constantly shut off [24]. This was corroborated in the *pdeR^{-A}* mutant macrocolony, which was fully unstructured and devoid of matrix (Fig. 3).

dgcM

Knocking out *dgcM* does eliminate not only its activation of MlrA by direct interaction but also the positive feedback loop by which DgcM-generated c-di-GMP feeds into the PdeH/DgcE-controlled c-di-GMP pool [24,27]. Consistent with this mechanism originally detected in liquid cultures, *dgcM* deletion strongly reduced the overall production of extracellular matrix also within macrocolonies, with the remaining matrix appearing in a highly heterogeneous manner across the upper macrocolony layer (Fig. 3c). This resulted in smaller, yet thicker macrocolonies with small intertwined wrinkles, which were similar to macrocolonies of strains that produce pEtN-cellulose only [12,16], but which clearly contrasted with the large and flat macrocolonies of the parental strain featuring the typically ordered and asymmetric internal matrix architecture and macroscopic patterns of radial ridges (Fig. 3a).

dgcM^{-A}

This mutant expresses a catalytically inactive variant of DgcM (DgcM^{-A}; with the GGEEF motif changed to GGAAF); that is, it lacks the positive feedback loop provided by DgcM-generated c-di-GMP. However, DgcM^{-A} is still able to bind to and stimulate the activity of MlrA [24]. This stimulatory effect of DgcM^{-A} on matrix synthesis was readily visible also in macrocolonies, as the *dgcM^{-A}* mutant formed large flat macrocolonies with radial ridges that contrasted with the small thick macrocolonies of the *dgcM* knockout mutant (Fig. 3a). The heterogeneous pattern of matrix distribution was in principle comparable to matrix architecture in the parental AR3110 macrocolony (Fig. 3c), suggesting that the positive feedback loop via DgcM-synthesized c-di-GMP plays a minor role only for matrix architecture in macrocolonies.

pdeR dgcM

Consistent with PdeR being the core element of the c-di-GMP-dependent switching mechanism, also

Fig. 3. Role of individual DGCs and PDEs in generating curli/pEtN-cellulose heterogeneity in *E. coli* macrocolony biofilms. (a) Top-view image of macrocolony biofilms of AR3110 and derivatives strains harboring single, double and/or specific point mutations in components of the *csgD*-controlling c-di-GMP signaling network. Macrocolonies were grown in salt-free LB medium supplemented with TS for 3 days. (b) Macrocolonies of respective strains shown in panel a were cryoembedded and sectioned perpendicular to the plane of the macrocolony at a thickness of 5 µm. Images are a combination of brightfield/fluorescence pictures that show the TS fluorescence pattern in thin sections of respective macrocolonies at low magnification. (c) Fluorescence, brightfield and merged images showing enlarged views of respective color-coded macrocolony areas boxed in panel b. Fluorescence images reveal the distribution and organization of TS-stained matrix in the upper layer of macrocolony biofilms.

this double mutant did not show local heterogeneity of matrix production (Figs. 3 and 4e). The absolute level of matrix was in fact comparable to that of a *pdeR* macrocolony; that is, in the absence of the inhibitor PdeR, not only the positive feedback loop via DgcM-produced c-di-GMP, but also the direct activator function of DgcM for MlrA is less effective than in the presence of PdeR, where this dual positive role of DgcM has been clearly shown both *in vivo* and *in vitro* [24]. This suggested that the regulatory circuitry involving PdeR, DgcM and MlrA may include an additional element not yet included in Fig. 2 (this issue is addressed further below).

In conclusion, this detailed analysis of macrocolony matrix architecture of various *pdeR* and *dgcM* mutants showed that (i) PdeR is the key component for generating local heterogeneity of matrix production in the intermediate macrocolony layer; (ii) DgcM's previously shown impact on matrix production, which operates via its direct interaction and activation of MlrA [24], may contribute to preventing PdeR from inhibiting MlrA (and thus becomes dispensable in the absence of PdeR); and (iii) the positive feedback loop provided by DgcM-synthesized c-di-GMP is of minor importance for macrocolony matrix architecture. While c-di-GMP input via the trigger PDE PdeR is crucial for generating local heterogeneity of matrix production, this input is not involved in generating the distinct matrix architecture of vertical pillars and the more horizontally connected network below the pillars,

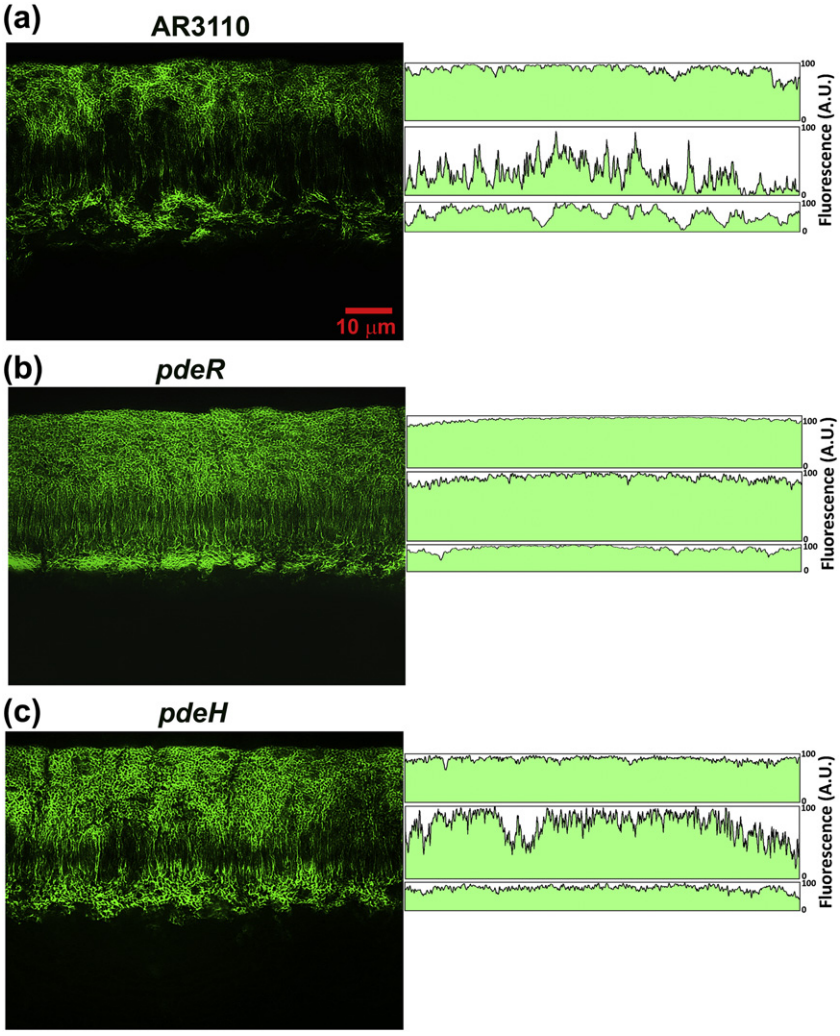

Fig. 4. High-resolution visualization and relative quantification of TS-stained matrix architecture in macrocolonies of the *E. coli* AR3110 strain and mutant derivatives lacking PDEs and DGCs with major roles in regulating matrix heterogeneity. Fluorescence images (left) are high-resolution versions of the corresponding images presented in Fig. 3c, which reveal the distribution and organization of TS-stained matrix in the upper layer of respective macrocolony biofilms in greater detail. The spectral plots (right) depict quantified patterns of TS fluorescence in three distinct zones within the upper layer of macrocolonies.

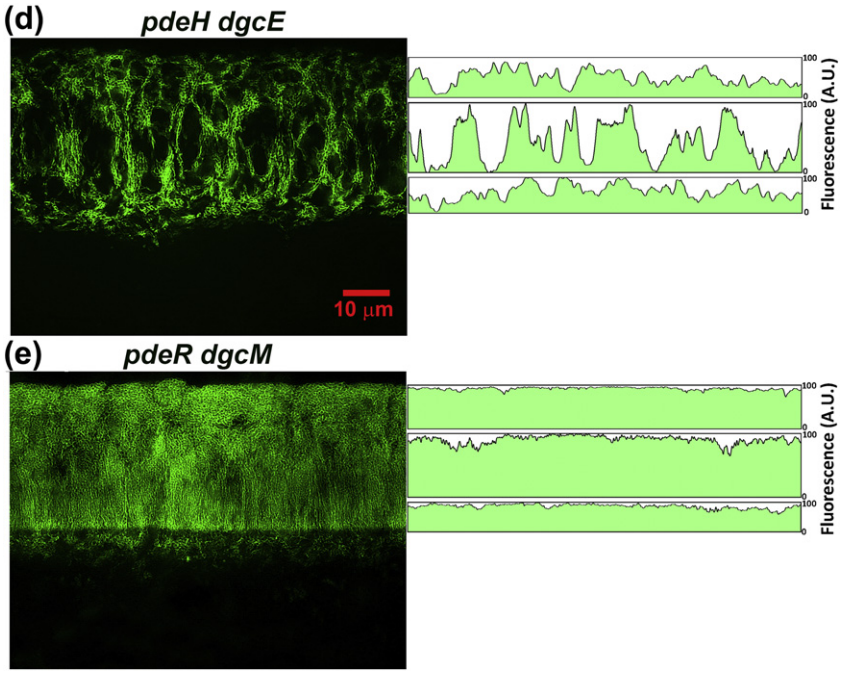

Fig. 4. (*continued*).

as this specific spatial arrangement persisted also in macrocolonies of *pdeR* or *pdeR dgcM* mutants (Fig. 4). Thus, this arrangement per se seems to reflect distinct spatial cell proliferation patterns in different biofilm zones rather than patterns of matrix production control.

The roles of the master PDE PdeH and the DGC DgcE in controlling matrix architecture via the PdeR/DgcM switch

The finding that c-di-GMP input via the PdeR/DgcM switch is crucial for establishing local matrix heterogeneity in macrocolony biofilms of *E. coli* raised the question of the roles of PdeH and DgcE, that is, the enzymes that antagonistically "negotiate" this c-di-GMP input [23,24].

pdeH

During growth and entry into stationary phase, PdeH is the master PDE of *E. coli* that maintains the cellular pool of c-di-GMP at a very low level (in a *pdeH* mutant, overall cellular c-di-GMP levels are about 10- to 15-fold higher) [33]. Consistent with its co-regulation with flagella, PdeH expression is very strong in the macrocolony bottom layer and becomes less and less pronounced further up into the intermediate zone [20]. As shown in Figs. 3c and 4c, *pdeH* mutant macrocolonies showed increased matrix production in the intermediate and upper layers, but the asymmetric overall architecture was not changed. Furthermore, matrix production was still heterogeneous in the intermediate layer, with small "dark" areas free of matrix still interspersed with the matrix "pillars." In short, knocking out *pdeH* leads to a quantitative increase in matrix production, while qualitative patterns remain unchanged.

dgcE

While knocking out *dgcE* hardly affects overall cellular c-di-GMP levels, DgcE provides for the major and specific c-di-GMP input into the PdeR/MlrA switch. Thus, *dgcE* deletion mutants express lower CsgD and curli expression during growth in liquid medium and show a macrocolony morphology that resembles that of a *dgcM* mutant or strains that express cellulose only [24,33]. This is corroborated here by the analysis of the matrix architecture (Fig. 3). The *dgcE* mutant still produced matrix heterogeneously, but absolute matrix amounts were significantly lower than in the parental macrocolony. Thus, with respect to macrocolony morphology and internal matrix architecture, *dgcE* and *dgcM* mutants show similar phenotypes.

pdeH dgcE

Knocking out both *pdeH* and *dgcE* eliminates the major players in the control of the c-di-GMP input into the PdeR/DgcM switching device. Interestingly, macrocolonies of *pdeH dgcE* double mutant revealed a clear qualitative change in matrix architecture. Pronounced

heterogeneity of matrix production could now be seen not only in the intermediate biofilm zone but also in the top stationary phase zone (Figs. 3 and 4d). Moreover, the stratified arrangement of matrix superstructures appeared to be *symmetric*, with the now heterogeneous top zone essentially replicating the appearance of the heterogeneous horizontal network of the matrix in the lower part of the intermediate macrocolony zone (as becomes especially clear in the quantifications in Fig. 4d; see also Fig. S1).

In conclusion, PdeH and DgcE exert an antagonistic quantitative influence on matrix production in macrocolonies, but are not involved in generating local matrix heterogeneity, which is the function of the PdeR/DgcM switch that operates just downstream of PdeH and DgcE. However, our analyses reveal that the interplay of PdeH and DgcE—with their different expression patterns along the vertical nutrient gradient and direct antagonistic roles in c-di-GMP control—is crucial to establish another qualitative feature of the spatial matrix architecture, that is, *asymmetry* in the vertical stratification of matrix patterns within the matrix-producing upper macrocolony layer. Thus, the differential expression of antagonistically acting PdeH and DgcE results in a large-scale spatial control of the c-di-GMP signal that biases the switch toward a CsgD/matrix^{ON} or CsgD/matrix^{OFF} state.

Heterogeneity and differential spatial organization of extracellular matrix in the upper layer of *E. coli* biofilms correlates with heterogeneity and differential expression levels of CsgD

As the c-di-GMP network that generates local heterogeneity of matrix production targets *csgD* transcription and the presence of CsgD is a prerequisite for expressing genes essential for both curli and pEtN-cellulose synthesis, *csgD* expression should spatially coincide with the distribution of matrix within the upper macrocolony layer. To evaluate this, macrocolonies of AR3110 carrying a merodiploid single-copy *csgD::gfp* reporter fusion were grown in the presence of Pontamine Fast Scarlet (P4B), a red fluorescent dye that like TS stains both pEtN-cellulose and curli without affecting the overall matrix architecture (Serra and Hengge, 2017), and then analyzed by cryosectioning and fluorescence microscopy. Consistent with CsgD being the key regulatory hub controlling matrix synthesis, the images reveal a precise spatial correlation between cells expressing *csgD* and producing matrix (Fig. 5). In the intermediate zone, vertically oriented chains of Gfp-expressing cells (i.e., cells in the CsgD^{ON} state) surrounded by P4B-stained matrix appeared interspaced with areas

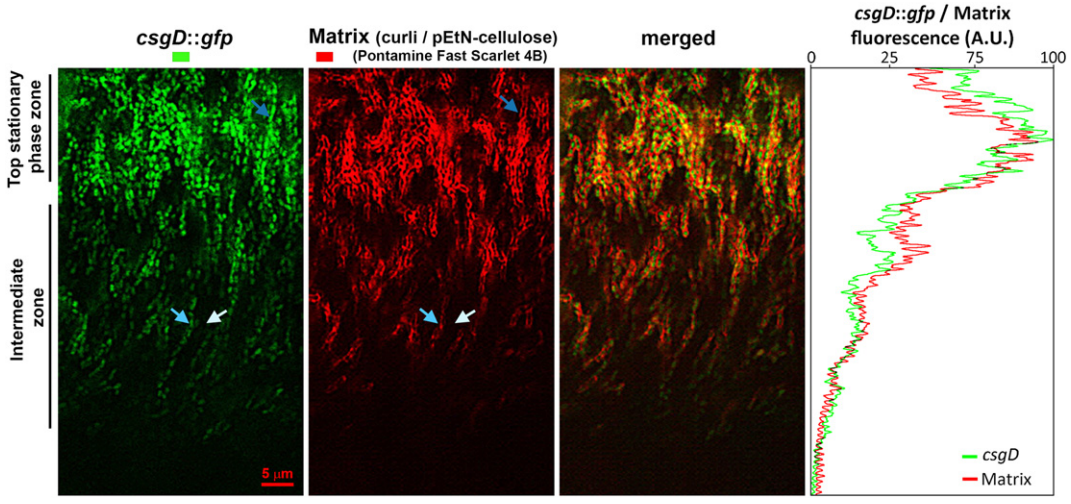

Fig. 5. Heterogeneity and spatial patterns of extracellular matrix in the upper layer of *E. coli* macrocolony biofilms correlate with heterogeneity and spatially controlled expression levels of the biofilm regulator CsgD. Macrocolonies of the AR3110 strain harboring a single-copy *csgD*::*gfp* fusion were grown in salt-free LB medium supplemented with Pontamine Fast Scarlet (P4B) for 3 days, cryoembedded and sectioned perpendicular to the plane of the macrocolony at a thickness of 5 µm. Thin sections were visualized by fluorescence microscopy using specific filters set to detect GFP and P4B fluorescence. The fluorescence image in the left panel shows the spatial pattern of CsgD expression across the upper macrocolony layer. The fluorescence image in the middle panel shows the corresponding pattern of P4B-stained matrix in the same thin section and position as presented in the left panel. The fluorescence image in the right panel results from merging the images shown in the left and middle panels. White, light blue and dark blue arrows indicate *E. coli* cells exhibiting CsgD^{OFF}/matrix^{OFF}, CsgD$^{ON(high)}$/matrix^{ON} and CsgD$^{ON(very\ high)}$/matrix^{ON} levels, respectively. The spectral plot (right panel) shows GFP and P4B fluorescence as a function of depth across the macrocolony cross section. The highest fluorescence intensity value was arbitrarily set to 100.

devoid of both Gfp and P4B fluorescence, with the latter representing cells that have not activated CsgD and thus also remain free of matrix. The chain-like alignment of $CsgD^{ON}$ cells suggests that once matrix synthesis has been switched on, this state is stably maintained in the progeny. Overall, this demonstrates that the local heterogeneity of extracellular matrix in the intermediate biofilm zone is based on heterogeneity of CsgD expression, that is, the parameter controlled by c-di-GMP via PdeH, DgcE and the PdeR/DgcM switch.

Notably, among cells in the $CsgD^{ON}$ state, distinct CsgD expression levels could be distinguished that were associated with the distinct patterns of matrix architecture found in the top and intermediate macrocolony zones (Fig. 5). Thus, cells densely surrounded by the curli/pEtN-cellulose nanocomposite in the top 'bricklayer'-like zone displayed clearly higher CsgD expression levels ($CsgD^{ON(very\ high)}$) than the chains of cells that generate the vertical matrix pillars in the intermediate zone ($CsgD^{ON(high)}$). This suggests that CsgD expression does not just occur in an all-or-none mode, but rather in a spatially fine-tuned manner that allows cells to display distinct CsgD levels across the upper macrocolony layer that ultimately contribute to different spatial matrix arrangements.

The *csgD*-controlling c-di-GMP signaling network generates heterogeneity of CsgD expression also in planktonic cultures during entry into stationary phase

Previous studies have shown that *E. coli* synthesizes matrix components also in liquid or planktonic culture when entering into stationary phase [12,22]. Moreover, the spatial order of physiological differentiation across macrocolony biofilms of *E. coli* parallels in part the nutrient-dependent temporal succession of the post-exponential and stationary-phase states in a planktonic culture [12,15,19,20]. Thus, we hypothesized that heterogeneity of CsgD expression may also occur in planktonic cultures.

To test this, expression patterns of CsgD along the growth curve of batch cultures were quantitatively analyzed by flow cytometry using the *E. coli* W3110 strain expressing the chromosomal *csgD::gfp* reporter fusion. As W3110 produces amyloid curli fibers (which in liquid culture diffuse away) [22], but is unable to synthesize pEtN-cellulose [12], cells of this strain are substantially less prone to aggregate, hence facilitating single cell analysis by flow cytometry. Notably, the absence of pEtN-cellulose does not feedback into CsgD regulation. Consistent with previous studies [20,23,30], CsgD expression was induced during the transition of cells from late post-exponential phase to early stationary phase (Fig. 6; this was about 10 h after starting the cultures, with the corresponding growth curves shown in Fig. S2). At 12 h, a bimodal distribution became evident, indicating that $CsgD^{ON}$ cells bifurcated into sub-populations expressing distinct CsgD levels. This bimodal pattern consolidated at 14 and 16 h, with a broad distribution of CsgD levels showing two clearly separate peaks. Thus, these $CsgD^{ON}$ subpopulations seem to correlate with those inhabiting the top and intermediate biofilm zones that also exhibited $CsgD^{ON(very\ high)}$ and $CsgD^{ON(high)}$ states, respectively. Overall, this demonstrates that heterogeneity of CsgD expression also occurs in planktonic cultures. In addition, it supports the results with macrocolonies showing that heterogeneity implies not only a diversification of cells in $CsgD^{OFF}$ and $CsgD^{ON}$ states, but also a distribution of $CsgD^{ON}$ cells into $CsgD^{ON(high)}$ and $CsgD^{ON(very\ high)}$ subpopulations.

To evaluate whether components of the c-di-GMP signaling network play equivalent roles in modulating CsgD/matrix heterogeneity in planktonic cultures and in macrocolonies, derivatives of *E. coli* W3110 carrying the *csgD::gfp* reporter fusion as well as the deletions or specific point mutations in the genes of this network were included in the flow cytometry analysis. None of the mutations had any effect on the growth patterns in batch cultures (Fig. S2). As expected, the *mlrA* mutant showed no induction of CsgD at all time points analyzed (defined as the $CsgD^{OFF}$ state marked by the vertical hatched red lines in Fig. 6). The *pdeR* mutant, which showed homogeneous matrix distribution in macrocolonies (Figs. 3 and 4), also exhibited induced and more homogenous CsgD expression in stationary phase (Fig. 6). Thus, PdeR plays the same crucial role in controlling CsgD/matrix heterogeneity in liquid cultures as in macrocolonies. Surprisingly, however, the high and narrow expression peak found for the *pdeR* mutant remained at the $CsgD^{ON(high)}$ level without further induction, thus corresponding to only one of the W3110 subpopulations (peaking at the green vertical lines in Fig. 6). This observation is further addressed below.

The *dgcM* and *dgcE* mutants showed unimodal distribution of CsgD expression with only partial induction never reaching the $CsgD^{ON(high)}$ state (Fig. 6), which agrees with the macrocolony phenotype of these mutants (Fig. 3). The $dgcM^{-A}$ mutant showed a CsgD expression pattern that at 14 and 16 h tended to approximate that of the parental strain, but with one histogram peak only that matched the $CsgD^{ON(high)}$ level and a long tail extending toward higher fluorescence intensity values. The differences between the $dgcM^{-A}$ and *dgcM* mutants confirmed that DgcM plays a positive role in CsgD expression, but that the DGC activity is dispensable, if not detrimental, for DgcM to stimulate high CsgD expression.

In the *pdeH* mutant, CsgD expression increased slightly earlier than in the parental W3110 strain with a large fraction of the entire population rapidly reaching the $CsgD^{ON(very\ high)}$ state at 12 h already. Even within this $CsgD^{ON(very\ high)}$ state, however, cells displayed a relatively broad distribution of expression levels. This

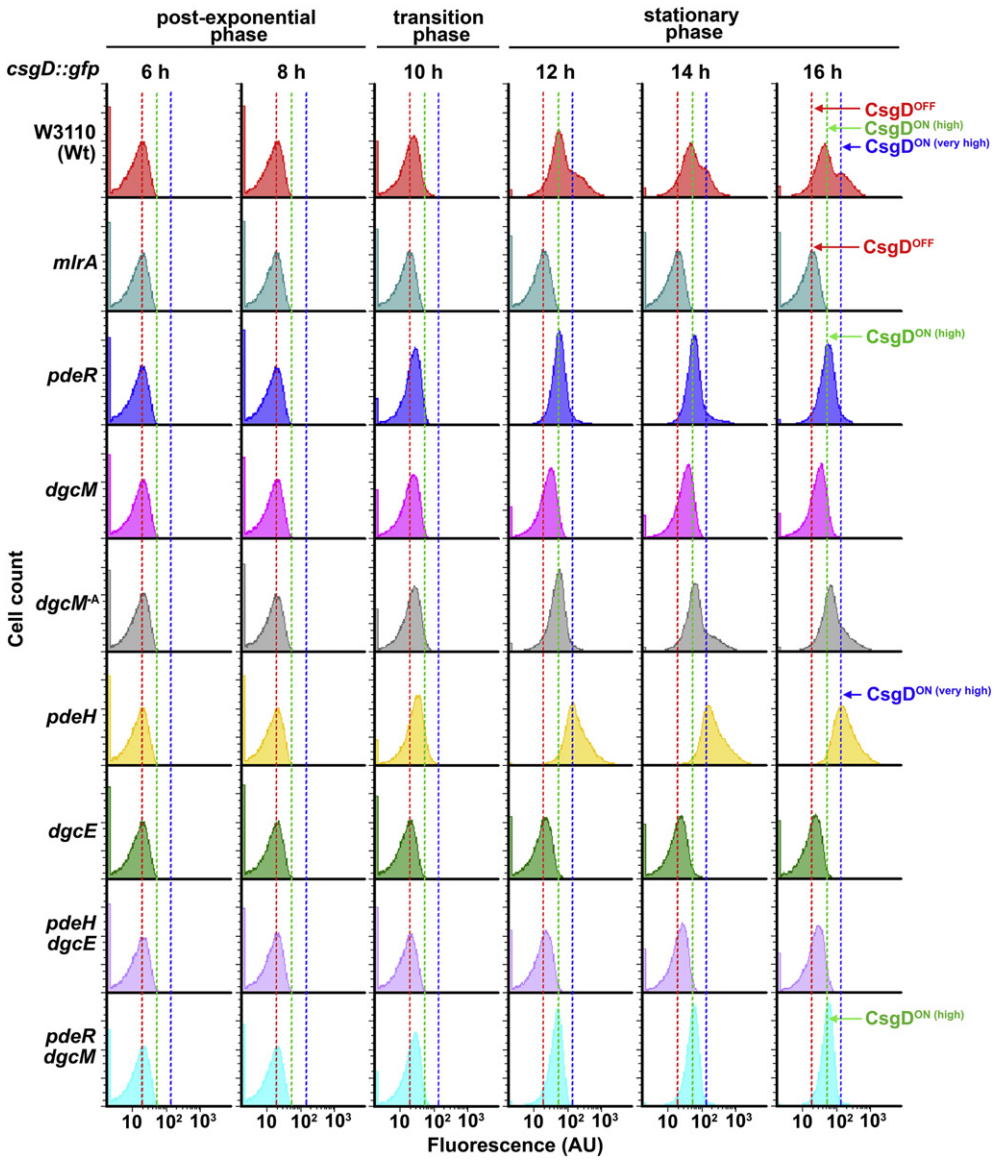

Fig. 6. Heterogeneity of CsgD expression also occurs in planktonic cultures and follows the same regulatory principles as in macrocolony biofilms. The *E. coli* W3110 strain and derivatives carrying the *csgD::gfp* reporter fusion as well as single-, double- and/or specific point mutations as indicated were grown as planktonic cultures at 28 °C, and cell suspensions of each strain were analyzed by flow cytometry at specific time points. The graphic presents histograms showing the distribution pattern of CsgD expression in cell populations of the different strains at distinct time points covering the indicated growth phases along the growth curve (see Fig. S2 for growth curves). The hatched red, green and blue lines indicate peak fluorescence intensities corresponding to the $CsgD^{OFF}$, $CsgD^{ON(high)}$ and $CsgD^{ON(very\ high)}$ states, respectively.

also agreed with the phenotypic behavior of *pdeH* macrocolonies, where matrix abundance increased significantly, but heterogeneity was still evident (Fig. 4c). The *pdeH dgcE* double-knockout showed a similar distribution of CsgD expression as the *dgcE* mutant with overall reduced CsgD activity, which emphasizes the important role of DgcE that may include a local signaling mechanism that cannot be substituted for by just higher cellular c-di-GMP levels as a consequence of knocking out *pdeH* [33].

Finally, the *pdeR dgcM* double-knockout mutant showed the same homogeneous pattern of CsgD expression as the *pdeR* mutant, with a somewhat higher and narrower histogram peak in stationary phase (Fig. 6), which agrees with the even slightly more homogeneous matrix arrangement in the macrocolonies of the double mutant (Fig. 4e). This confirms that in the absence of PdeR, DgcM contributes hardly to enhance the activity of MlrA. Moreover, MlrA alone—in the absence of both PdeR and DgcM—can drive *csgD* transcription to the $CsgD^{ON(high)}$ state

(peaking at the green vertical line). However, in order to reach the CsgD$^{ON(very\ high)}$ state (the blue vertical line and beyond), the complex input of PdeR/DgcM into MlrA activity is crucial. Details of this input are addressed in the following section.

Overall, the results shown in Fig. 6 demonstrate that CsgD/matrix heterogeneity is not only found in non-spatially structured planktonic cultures as well, but that it is generated by the same mechanisms both in macrocolony biofilms and planktonic cultures.

In the absence of PdeR, the production of c-di-GMP by DgcM becomes a negative factor for maximal CsgD expression and matrix production

In the absence of both PdeR and DgcM, MlrA alone can drive CsgD production to the CsgD$^{ON(high)}$ state, but not beyond (Fig. 6). But why does the *pdeR* mutant—in which DgcM is intact—not induce CsgD further? The finding that CsgD expression in the *dgcM*$^{-A}$ mutant essentially corresponds to that of the parental wild-type strain (Fig. 6) suggested that DgcM's direct interaction with MlrA but not its DGC activity is required for stimulating MlrA activity—could it be that its DGC activity eventually becomes inhibitory in the absence of PdeR?

In order to test this, we introduced the *dgcM*$^{-A}$ allele into the *pdeR* knockout mutant carrying the *csgD*::*gfp* fusion and analyzed the CsgD expression pattern by flow cytometry (Fig. 7a). Strikingly, in this *pdeR dgcM*$^{-A}$ mutant, CsgD induction started extremely early, in fact already in post-exponential phase (8 h), which contrasted not only with CsgD induction in the parental strain but also with all other mutants analyzed (compare to the patterns in Fig. 6). Already at 10 h, the *pdeR dgcM*$^{-A}$ histogram showed a single high and narrow peak—that is, very homogeneous expression—that had passed the CsgD$^{ON(high)}$ line. At 12 h, the cell population mostly reached the CsgD$^{ON(very\ high)}$ status, with a histogram tail emerging toward even higher expression levels (Fig. 7a). Within macrocolonies, the *pdeR dgcM*$^{-A}$ mutant showed not only a highly homogenous pattern of TS-stained matrix across the upper layer but even some patches of matrix in the bottom layer (Fig. 7b), which fully agrees with flow cytometry data showing CsgD being expressed already in the late post-exponential phase in this mutant.

Overall, the flow cytometry data with the *pdeR dgcM*$^{-A}$ mutant reveal an intriguing fine regulation of CsgD expression by PdeR/DgcM. Single-deletion mutations in either *pdeR* or *dgcM* clearly show the overall inhibitory or activating functions, respectively, of these components in MlrA-mediated CsgD expression (Fig. 6). However, comparing CsgD expression patterns in the *pdeR dgcM*$^{-A}$ and the *pdeR* mutants surprisingly revealed a *negative* effect of DgcM's DGC activity *in the absence* of PdeR (Figs. 6 and 7).

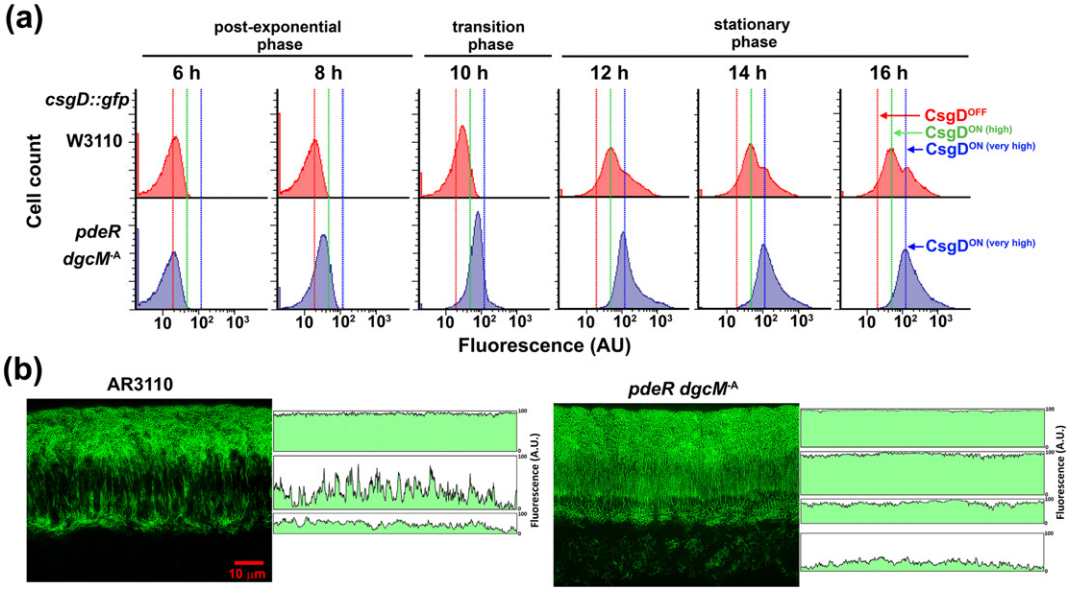

Fig. 7. In the absence of PdeR, the catalytically inactive DgcM^{-A} variant drives maximal constitutive CsgD expression and matrix production in *E. coli* biofilms. (a) The *E. coli* W3110 strain and its *pdeR dgcM*$^{-A}$ derivative carrying the *csgD::gfp* reporter fusion were grown in planktonic cultures at 28 °C, and at specific time points, cell suspensions of each strain were analyzed by flow cytometry. The graphic presents histograms showing the distribution pattern of CsgD expression in cell populations of both strains at distinct time points and growth phases along the growth curve. The red, green and blue lines indicate peak fluorescence intensities corresponding to CsgD^{OFF}, CsgD$^{ON(high)}$ and CsgD$^{ON(very\ high)}$, respectively. (b) Fluorescence images reveal the distribution and organization of TS-stained matrix in AR3110 and *pdeR* DgcM^{-A} macrocolony biofilms, as quantified by the adjacent spectral.

Loss of heterogeneity in extracellular matrix production results in severe disruption of *E. coli* macrocolony biofilms during macroscopic buckling and folding

Why does *E. coli* use such a strikingly elaborate mechanism for heterogeneous matrix production in certain biofilm zones? What is the physiological adaptive value of this local heterogeneity for the biofilm community? The obvious and readily visible impact is on biofilm morphology. Macrocolonies of mutants with homogenous and/or overall increased matrix production (i.e., *pdeR*, *pdeR dgcM*, *pdeR dgcM*$^{-A}$, *pdeH*) are larger and flatter and show fewer ridges than macrocolonies of the parental strain AR3110 (Figs. 3a and 9a). This phenotype is obviously a consequence of increased matrix and therefore increased cohesion in the upper layer, which makes upper layer buckling and folding more difficult and thus less frequent, thereby enforcing further horizontal radial expansion of the macrocolonies.

At microscopic resolution, changes in the supracellular architecture of the ridges, which were still occasionally formed by macrocolonies with homogenous matrix distribution, became apparent. Unlike the ridges of macrocolonies of strains showing matrix heterogeneity (AR3110 and the *pdeH* or *pdeH dgcE* mutants), ridges formed by the *pdeR*, *pdeR dgcM* and *pdeR dgcM*$^{-A}$ macrocolonies were thinner with narrow tips and showed a single and highly homogeneous pattern of matrix organization, with extremely small round cells surrounded by massive amounts of extracellular matrix (Fig. 8a). Furthermore, scanning electron microscopy (SEM; Fig. 8b) showed that the surface of a 6-day-old *pdeR* mutant macrocolony exhibited many microfissures and larger breaks, in particular also along the top of the ridges. Most bacteria in the interior faces of these ruptures were fully covered with extracellular matrix, consistent with the matrix patterns seen in TS-stained cryosections of *pdeR* mutant macrocolonies (Figs. 4b and 8a).

Based on these findings, which indicate an impact of matrix architecture on elastic colony behavior, entire macrocolonies of AR3110 and the various matrix-affected mutants were visually examined during growth over extended times. Until day 6, macrocolonies of all strains grew without macroscopic evidence of damage in overall structure (Fig. 9). However, by day 10, macrocolonies with homogenous matrix distribution (i.e., of *pdeR*, *pdeR dgcM*, *pdeR dgcM*$^{-A}$ mutants) became disrupted along multiple irregular lines that represent failed attempts to buckle up into ridges. In addition, larger elongated breaks and even holes followed the lines of the few ridges that had folded up earlier (Fig. 9). Interestingly, macrocolonies of the *pdeH* mutant with their increased, but still heterogeneous matrix production showed no apparent damage. Thus, it is the loss of local heterogeneity rather than the absolute increase in matrix that reduces elasticity and thus impairs biofilm integrity during folding. Overall, matrix heterogeneity seems to confer to macrocolony biofilms the optimal balance of cohesiveness and elasticity required to withstand the forces generated by local growth and buckling and thus to form and then preserve ridges and wrinkles with intact surfaces.

Discussion

Local matrix heterogeneity in macrocolony biofilms is generated by the c-di-GMP-triggered PdeR/DgcM switch that controls MlrA activity in *csgD* transcriptional activation

Long-range heterogeneity of CsgD and thus extracellular matrix production in macrocolonies of *E. coli* have long been known to follow nutrient gradients with a stratification into distinct physiological states characterized by different genome-wide gene expression patterns [12,15,19,20]. With *Salmonella enterica*, which exhibits similar CsgD regulation, macrocolony homogenization and FACS analysis or just physical separation of clustering and non-clustering subpopulations also showed heterogeneity of CsgD expression [34,35]. By contrast, our study presented here has addressed the question of the mechanistic origin and physiological function of short-range, that is, local heterogeneity of CsgD/matrix production *in situ*, in directly adjacent cell clusters that experience similar external conditions within macrocolony biofilms (Fig. 1). Here, not only the underlying regulatory mechanisms have been clarified, but we have also shown that this heterogeneity occurs and is elicited by the same mechanisms in planktonic culture as well and thus does not represent a biofilm-specific regulatory behavior.

Our genetic analysis demonstrates that PdeR, a "trigger" PDE [24,27], is the key component of a switch that generates this local heterogeneity of matrix production. Switching relies on PdeR occurring in two different states (Fig. 2): (i) PdeR can directly interact with both DgcM and MlrA, thereby inhibiting c-di-GMP synthesis by DgcM and transcriptional activation at the *csgD* promoter by the DgcM/MlrA complex; alternatively, (ii) PdeR can bind and degrade c-di-GMP (provided by DgcE), which results in a release of DgcM and MlrA from PdeR, allowing DgcM to generate c-di-GMP and DgcM/MlrA to activate *csgD* transcription [24,27]. Heterogeneity of CsgD and matrix production thus reflects PdeR being in one or the other state.

The PdeR/DgcM/MlrA circuitry (Fig. 2) contains nested double-negative feedbacks, that is, network motifs classically associated with regulatory switches [1,6,36–38]: (i) PdeR degrades the c-di-GMP which prevents it from inhibiting DgcM and MlrA, and (ii) DgcM inhibits (via c-di-GMP synthesis) its own

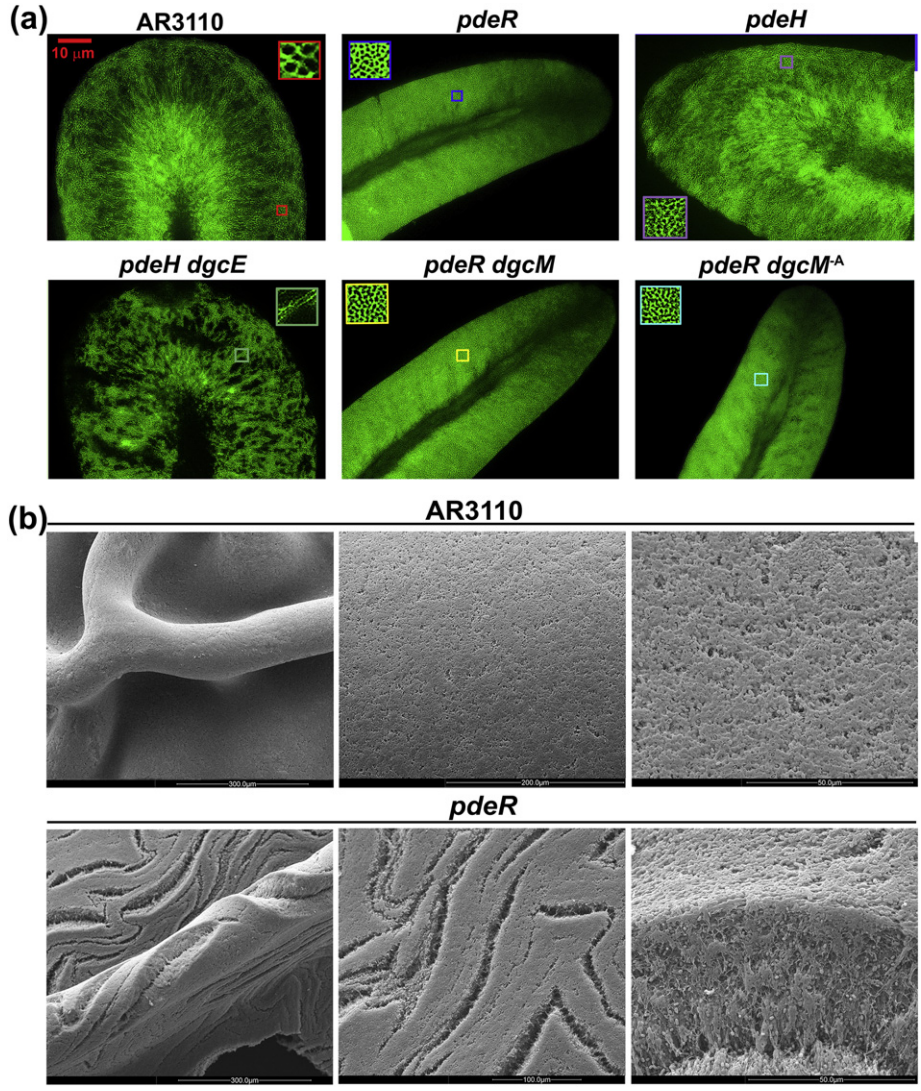

Fig. 8. Homogeneously produced extracellular matrix alters the supracellular architecture of ridges and causes a loss of structural integrity of *E. coli* macrocolony biofilms. (a) High-resolution fluorescence images of sections through the tips of ridges of mature macrocolonies are shown for strain AR3110 and the indicated mutant derivatives. The insets show enlarged views of the color-boxed areas in the respective images, which show well-defined bacterial silhouettes for all strains. Note that bacterial silhouettes outlined by matrix in *pdeR*, *pdeR dgcM* and *pdeR dgcM*$^{-A}$ ridges are round and substantially smaller than those in the AR3110 ridge. (b) Top-view SEM images (at different magnifications) of representative surface areas of 6-day-old macrocolonies of strain AR3110 and its *pdeR* mutant derivative. Unlike the AR3110 biofilm, the *pdeR* macrocolony exhibits numerous microfissures in its surface. Bacteria in the interior faces of these microfissures appear mostly covered with extracellular matrix (bottom right panel).

inhibitor PdeR or vice versa (PdeR inhibiting c-di-GMP synthesis by DgcM). *In-silico* modeling indeed showed this circuitry to have the potential to act as a bistable switch [28], a property that our *in vivo* and *in situ* analysis presented here demonstrates to be crucial for generating local CsgD/matrix heterogeneity in the intermediate zone of macrocolony biofilms. In this biofilm zone, the intracellular c-di-GMP input into PdeR thus seems to be within a range that allows PdeR to switch into either one or the other state. Establishing this range of c-di-GMP input is achieved by spatial control along the vertical nutrient gradient, which inversely affects the expression of PdeH and DgcE, that is, the enzymes that antagonistically "negotiate" this c-di-GMP input [20] (as discussed further below).

A novel fine-tuning homeostatic feedback loop in the molecular function of DgcM in controlling MlrA activity

DgcM is an important accessory component with a positive impact on the MlrA-mediated activation of

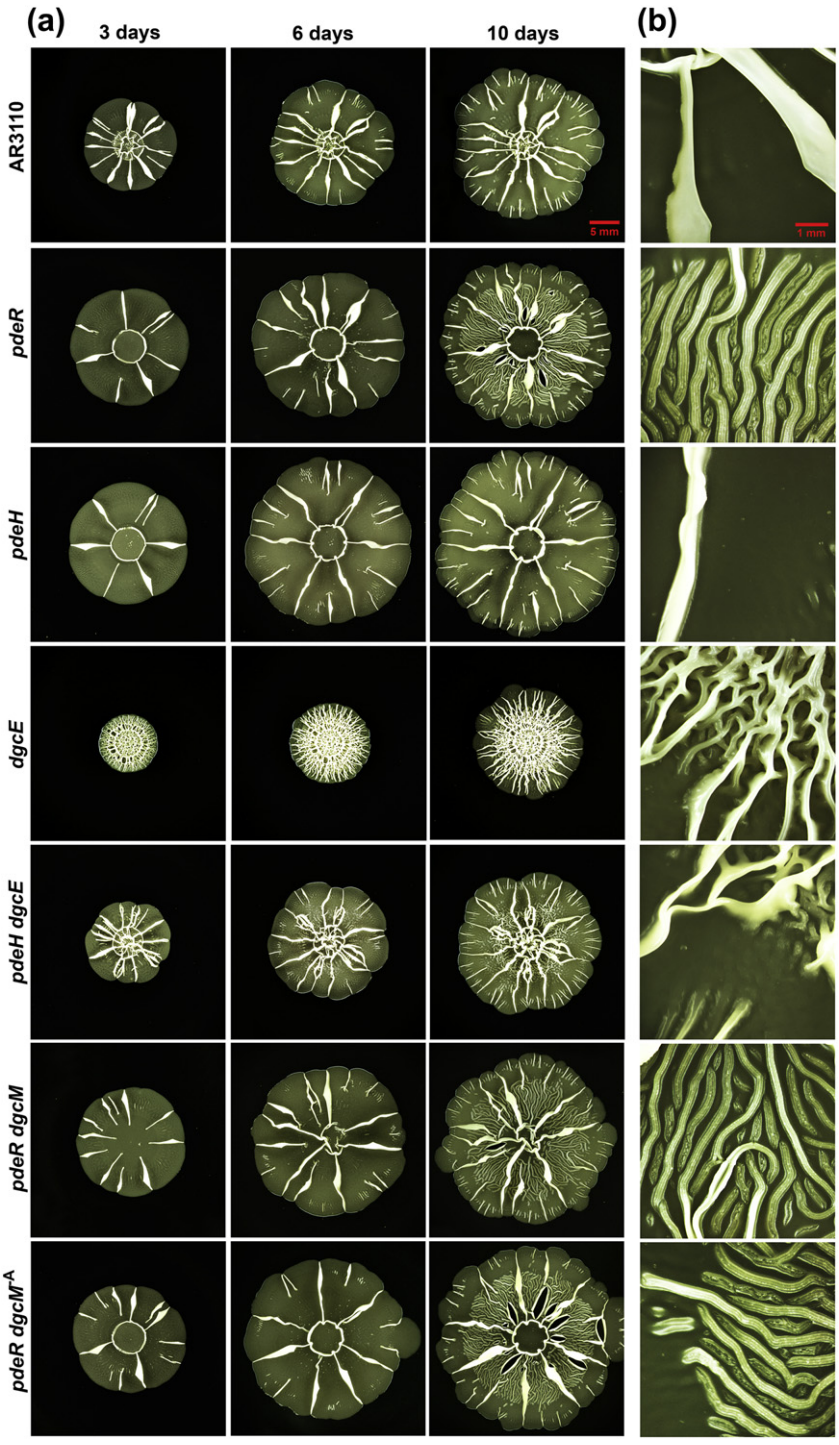

Fig. 9. During long-term growth, the absence of heterogeneity in extracellular matrix production in the intermediate layer leads to severe damage in the upper layer of *E. coli* macrocolony biofilms. (a) Top-view images of macrocolony biofilms of AR3110 and the indicated mutant derivatives at days 3, 6 and 10 after inoculation. Macrocolonies were grown in salt-free LB agar plates supplemented with TS at 28 °C. By day 10, elongated ruptures and larger breaks in the upper layer of macrocolonies became macroscopically apparent. (b) Magnified view of a representative region of the respective macrocolonies at day 10 presented in panel a.

transcription at the *csgD* promoter [22–24,33]. Our results shown here shed new light on the mechanism by which DgcM activates MlrA and, in addition, reveal a complex fine-tuning homeostatic feedback also operating at the level of DgcM.

In a wild-type background, that is, in the presence of PdeR, the major activating effect of DgcM on MlrA-dependent CsgD expression does not depend on DgcM's ability to produce c-di-GMP (compare wild-type, *dgcM* and *dgcM*$^{-A}$ strains in Fig. 6). This seems to suggest that DgcM activates mainly by its direct interactions (with MlrA and/or PdeR) and that the positive feedback loop via its local c-di-GMP production that contributes to prevent PdeR from binding and inhibiting DgcM and MlrA is of minor importance. However, the data with strains lacking PdeR indicate that the regulatory interplay is even more complex. In the absence of PdeR, the presence or absence of DgcM makes hardly any difference for CsgD expression patterns (Fig. 6), indicating either that DgcM activates MlrA mainly by "fending off" PdeR by direct interaction (rather than being a true co-activator for MlrA despite its ability to interact with MlrA), or that DgcM is somehow self-inhibitory if PdeR is not around. The data obtained with the catalytically inactive DgcM^{-A} variant in the *pdeR* mutant background (Fig. 7) clearly point to the second of these two possibilities. In the absence of PdeR, this DgcM variant, which does not produce c-di-GMP, was found to superactivate MlrA, with CsgD expression starting earlier (already between 6 and 8 h) and being stronger than in any other strain (compare the *pdeR dgcM*$^{-A}$ strain to the wild-type in Fig. 7 and to the *pdeR* and *pdeR dgcM* mutants in Fig. 6). This allows two conclusions: (i) DgcM definitely is a direct co-activator for MlrA (and not just keeps the inhibitor PdeR out of the way), and (ii) DgcM's own DGC activity becomes inhibitory in a configuration where PdeR is absent and *csgD* transcription is controlled solely by the interplay between DgcM and MlrA. Mechanistically, this could mean that DgcM-produced c-di-GMP—by binding either to DgcM's I-site or to MlrA—reduces the propensity for DgcM/MlrA interaction, which promotes transcriptional initiation at the *csgD* promoter. C-di-GMP acting via the I-site of DgcM seems more likely, since the I-site clearly binds c-di-GMP (which, however, does not inhibit DGC activity; i.e., this I-site has been in search of a function), whereas no specific c-di-GMP binding to MlrA could be observed in extensive *in vitro* assays [24]. There is, however, a third alternative scenario: it could also be DGC activity of DgcM per se, that is, structural nanomovements associated with the catalytic process itself, that somewhat destabilize its interaction with MlrA; if so, also DgcM would be a trigger enzyme, that is, a protein whose regulatory interaction with another—output-generating—macromolecule is affected by its own substrate binding and catalytic activity [24,27,39]. Future experiments will have to distinguish between these "I-site" and "trigger enzyme" scenarios. Finally, this negative effect of DgcM-produced c-di-GMP becomes apparent in the *pdeR* mutant, but not in PdeR-proficient strains. This indicates that PdeR—via its PDE activity—counteracts this inhibitory effect. Thus, integrated within the principal circuitry (Fig. 2), in which PdeR and DgcM—via their direct interactions with each other and with MlrA—act as direct inhibitor and activator, respectively, there seems to be an intricate c-di-GMP-based homeostatic fine-tuning loop, in which DgcM assumes a negative role, whereas PdeR contributes positively to DgcM/MlrA-mediated *csgD* transcription.

Antagonistic c-di-GMP control by differentially expressed PdeH and DgcE generates the long-range vertical asymmetry of the stratified matrix architecture within macrocolony biofilms

c-di-GMP-mediated input into the PdeR/DgcM switch is provided by the antagonistically acting enzymes PdeH and DgcE [23,24]. PdeH is the most abundant and highly active c-di-GMP-degrading PDE in *E. coli*, which maintains a very low cellular c-di-GMP level (which in liquid culture does not exceed 80–100 nM, even under conditions where c-di-GMP-dependent processes such as matrix production are activated; knocking out *pdeH* increases this level to approx. 1 μM). This draining of the pool by the master PDE PdeH (to levels clearly lower than the K_d's for c-di-GMP binding of the effectors) allows and restricts distinct DGCs to locally and in parallel activate different effector/target systems in their immediate vicinity within larger protein complexes [33]. Two systems have been shown to be strongly affected by knocking out *dgcE*, that is, inhibition of flagellar rotation by the c-di-GMP-binding "brake" protein YcgR [40–42] and the PdeR/DgcM switch that controls MlrA activating *csgD* transcription [23,24]. The already very low cellular c-di-GMP pool is hardly affected by a *dgcE* mutation, and the observed interaction between DgcE and PdeR suggests a not yet further characterized local signaling between these factors [33]. Nevertheless, the antagonistic activities of the dominant PdeH and DgcE act additively, as can be seen in the *pdeH* mutant background, where the 10- to 15-fold higher c-di-GMP level is reduced again when a secondary deletion of *dgcE* is introduced, but still remains 3- to 4-fold higher in the double mutant than in the parental wild-type strain [24,33].

Our *in situ* analysis in macrocolony biofilms showed that single knockouts of either *pdeH* or *dgcE* generate more or less matrix, respectively, with local heterogeneity of matrix production still preserved (Figs. 3 and 4). However, the analysis of the *pdeH dgcE* double mutant revealed an intriguing function of the interplay between PdeH and DgcE in qualitatively controlling

matrix architecture. In contrast to macrocolonies of the parental wild-type strain, which show an asymmetric architectural stratification within the matrix-producing upper layer (Fig. 1), the *pdeH dgcE* double mutant displayed a symmetric arrangement, where the very top zone no longer featured a homogeneous "dense brickwork"-like matrix arrangement, but essentially looked similar to the "loose horizontal network" present in the lowest stratum of the matrix-producing layer, as became clearly apparent in the flat macrocolony areas (Figs. 4d and S2) as well as in the tips of the ridges (Fig. 8a).

This means that the complex vertical asymmetry of the matrix architecture is the result of a continous shift in the c-di-GMP balance established by PdeH and DgcE along the biofilm *z*-axis over the long-range distance of 40–45 μm. This is clearly a reflection of the vertical nutrient gradient, which differentially controls PdeH and DgcE expression. Thus, *pdeH* is under control of the flagellar transcriptional control cascade (FlhDC/σ^{FliA}) [43], with expression being very high in the postexponentially growing cells in the *lower* zones and fading out in the upper zones of macrocolony biofilms [20,29], whereas *dgcE* is induced by the stationary phase sigma factor σ^{S} [31], which is itself induced and activated in the starving *upper* cell layer [20]. As a result, the PdeH/DgcE-negotiated input into the PdeR/DgcM switch is dominated by DgcE in the uppermost zone, thus driving a very high fraction of cells into very high CsgD/matrix production, which generates the nearly homogeneous "dense brickwork"-like matrix architecture. In the lower matrix-producing zones, however, the result of the PdeH/DgcE interplay is in the range that allows for bifurcation in PdeR/DgcM switch behavior and thus heterogeneous matrix production.

Currently, it is unknown whether this long-range PdeH/DgcE-dependent spatial shift in the c-di-GMP balance in macrocolonies affects the global c-di-GMP pool in individual cells or whether at the cellular level this remains a local c-di-GMP signaling phenomenon as in planktonic cells that maintain the very low cellular c-di-GMP concentration also in later stationary phase despite the disappearance of PdeH [33], where another PDE may take over the role of the master PDE keeping overall c-di-GMP levels low. In order to distinguish between these possibilities, high-sensitivity visual reporters of cellular c-di-GMP levels appropriate to *in situ* analysis in cryosectioned biofilms will have to be developed.

The physiological role of local matrix heterogeneity: generating elasticity that allows biofilms to buckle up and fold without breaking

Why has *E. coli* evolved such an intriguingly complex c-di-GMP-based regulatory network as described above that allows a community of billions of bacterial cells to build and control an intricate matrix architecture on a scale that is almost 2 orders of magnitude larger than individual cells (a relationship that is intriguingly similar to that between individual humans and a gothic cathedral)? What is the adaptive value for the *E. coli* biofilm community of all this effort in building this matrix architecture? We could demonstrate here that eliminating matrix heterogeneity in the intermediate zone of macrocolonies (in all single or double mutants that lack *pdeR*) impaired mechanical properties, that is, the tissue-like elasticity required to maintain integrity of entire macrocolonies during buckling and folding. This became evident by initial microfissures and then by larger elongated fractures and even holes breaking up in the surface of those macrocolonies. Also, fewer and equally cracking ridges can be observed, indicating that the elongated microfissures on the macrocolony surface represent failed attempts to buckle up and fold into ridges. A physiological benefit of avoiding such fractured and disrupted biofilm surfaces in natural environments seems obvious—smooth and evenly matrix-covered outer surfaces are likely to maintain appropriate humidity and homeostatic conditions in general as well as to prevent microbial predators or fungal hyphae from penetrating into the biofilm.

At a more mechanistic level, why is matrix heterogeneity in the intermediate macrocolony zones, that is, the maintenance of adjacent cellular subpopulations that either produce matrix or do not, so crucial for large-scale elasticity, that is, the ability of macrocolonies to resist mechanical stress that maximally arises in the curvatures that occur during buckling and folding? We propose here that these two subpopulations represent a case of division of labor. The matrix-producing cells are fixed at their place and build up the large-scale matrix architecture that like an internal skeleton allows macrocolony biofilms to grow into stable macroscopic structures (note that ridges have a width of approximately 90–100 μm, but can rise to be >5 mm high—a ratio that in human dimensions corresponds to a 5-m-high wall of a base width of only 10 cm). By contrast, the non-matrix producing cells between the vertical matrix pillars and horizontal matrix network in the intermediate biofilm layer get flexibly pushed around from compressed to stretched areas during microscopic growth and macroscopic folding of tissue-like macrocolony biofilms. This passive cellular movement would dissipate stress and avoid the formation of voids and internal disruptions that could interfere with capillary action required for maintaining necessary fluxes of water, nutrients and other compounds. Overall, this division of labor is the basis of the collective building of the intricate supracellular matrix architecture and the biomechanical properties that maintain biofilm integrity and allow for the amazing macroscopic morphogenesis of wrinkling biofilms growing at humid and nutrient-providing surface-air interfaces.

Materials and Methods

Bacterial strains and growth conditions

All strains used are derivatives of the *E. coli* K-12 strains W3110 [44] or the direct W3110-derived strain AR3110, in which codon 6 in the chromosomal copy of *bcsQ* (a stop codon TAG in the cellulose-negative W3110) was changed to the sense codon TTG that is present in other cellulose-proficient *E. coli* strains [12]. The construction of the chromosomal single copy *csgD*::*gfp* reporter fusion inserted into the phage lambda *att* site in strains W3110 and AR3110 was previously described [12,20]. Knockout mutations in *pdeH* (*yhjH*), *dgcE* (*ygcE*), *pdeR* (*yciR*), *dgcM* (*ydaM*) and *mlrA* are full *orf* deletion/resistance cassette insertions generated in W3110 and were previously described [22,23]. Point mutations in the $pdeR^{-A}$ (EAL-to-AAL) and $dgcM^{-A}$ (GGEEF-to-GGAAF) alleles in the W3110 chromosomal background were also described previously [24]. The $bcsQ^{+}$ allele of strain AR3110 was transferred into W3110 derivatives harboring knockout or point mutations using a *kan* insertion cassette located between *dppF* and *yhjV* for P1 co-transduction. The *kan* cassette was subsequently flipped out [45]. Between the W3110 and AR3110 backgrounds, mutations with selectable markers were transferred by P1 transduction [46].

Growth of bacterial macrocolonies

Bacterial cells were grown overnight in liquid LB medium under aeration at 37 °C. Five microliters of the overnight cultures was spotted on salt-free LB agar plates. Where indicated, these plates were supplemented with TS (40 μg ml^{-1}) or Pontamine Fast Scarlet (P4B, 40 μg ml^{-1}), which show green and red fluorescence, respectively, upon binding to pEtN-cellulose and amyloid curli fibers [12,47]. Plates with macrocolonies were incubated at 28 °C for the indicated periods of time. Growth below 30 °C is required for matrix production since expression of CsgD is temperature-sensitive in *E. coli* K-12 strains [22,48]. The resulting macrocolony biofilms are very large (diameter of ~20 mm after 5 days) and extremely flat (only ~60 μm along the vertical *z*-axis) and from the second day of growth on buckle up and fold into macroscopic ridges and smaller wrinkles.

Stereomicroscopy

E. coli macrocolony biofilms were visualized at ×10 and ×50 magnification with a Stemi 2000-C stereomicroscope (Zeiss, Oberkochen, Germany). Digital images were captured with an AxioCam-ICC3 digital camera coupled to the stereomicroscope, operated via the AxioVision 4.8 software (Zeiss).

Cryosectioning of macrocolony biofilms and fluorescence microscopy

The procedure and materials used to cryosection macrocolony biofilms and to further examine and visualize TS, P4B or GFP fluorescence in cross-sections were exactly as described previously [12,47]. When indicated, TS fluorescence and brightfield images were superimposed using Adobe Photoshop CS6 in order to show the fluorescence location on the biofilm section. Similarly, P4B and GFP fluorescence images were superimposed to show location of matrix and *csgD::gfp* expression, respectively. Quantification of the spatial distribution of TS/P4B-stained matrix or CsgD::Gfp in interior zones of macrocolony biofilms was performed using Fiji (ImageJ) software. Zones in cross-section images were selected using the ROI manager, and spectral plots were generated using the Multi Plot command. Fiji-generated plots were scaled to the size of respective selected areas in macrocolony cross-section images. The fluorescence intensity range in individual plots was arbitrarily set to 0–100.

Scanning EM of bacterial macrocolonies

Preparation and SEM analysis of macrocolony biofilm samples was performed exactly as described previously [15].

Flow cytometry

Bacterial cells were grown overnight in liquid LB medium at 37 °C under agitation. Overnight-grown bacteria were inoculated to an initial OD_{578} of 0.05 in salt-free LB and incubated at 28 °C with agitation to allow bacterial growth. At indicated time points, an aliquot of each cell suspension was harvested and fixed in 10% neutral buffered formalin for 5 min. After fixation, cells of each sample were washed twice with phosphate-buffered saline buffer, diluted in phosphate-buffered saline buffer and vortex-mixed to ensure disaggregation of cell clumps. The absence of cell aggregates was confirmed by light microscopy and flow cytometry using forward scatter and side scatter parameters. Cell samples were subjected to flow cytometry analysis using a Becton Dickinson (BD) Accuri C6 device. Data were captured using the BD Accuri C6 software. GFP fluorescence was detected in FL-1 using a 510/15 BP filter. For each cell sample, at least 20,000 events were analyzed. Date were further analyzed using the FCS express 6 software (De Novo software). Figures were prepared using FCS express 6 and Adobe Photoshop CS6.

Acknowledgments

We thank Jens Rolff (Freie Universität Berlin) for the possibility to perform scanning EM in his laboratories.

This work was supported by the Deutsche Forschungsgemeinschaft (DFG grants He1556/17-1 and He1556/20-1, with the latter being part of DFG Priority Programme 1617 "Phenotypic heterogeneity and sociobiology of bacterial populations", both awarded to R.H.).

Author Contributions: Conceptualization of the study: both authors; experiments, data visualization and curation: DOS; formal analysis of data: both authors; supervision, project administration, funding acquisition: RH; writing: both authors.

Declaration of Interest: None.

Appendix A. Supplementary data

Supplementary data to this article can be found online at https://doi.org/10.1016/j.jmb.2019.04.001.

Received 24 January 2019;
Received in revised form 26 March 2019;
Accepted 1 April 2019
Available online 4 April 2019

Keywords:
biofilm;
bacterial cellulose;
c-di-GMP;
CsgD;
curli

Current address: D.O. Serra, Instituto de Biología Molecular y Celular de Rosario (IBR), Universidad Nacional de Rosario—CONICET, Ocampo y Esmeralda, 2000 Rosario, Argentina.

Abbreviations used:
pEtN, phosphoethanolamine; TS, thioflavin S; PDE, phosphodiesterase; DGC, diguanylate cyclase; SEM, scanning electron microscopy.

References

[1] T.S. Gardner, C.R. Cantor, J.J. Collins, Construction of a genetic toggle switch in *Escherichia coli*, Nature 403 (2000) 339–342.
[2] D. Dubnau, R. Losick, Bistability in bacteria, Mol. Microbiol. 61 (2006) 564–572.
[3] J.-W. Veening, W.K. Smits, O.P. Kuipers, Bistability, epigenetics, and bet-hedging in bacteria, Annu. Rev. Microbiol. 62 (2008) 193–210.
[4] J. van Gestel, H. Vlamakis, R. Kolter, Division of labor in biofilms: the ecology of cell differentiation, Microbiol. Spectr. 3 (2015), MB-0002-2014.
[5] A. Dragos, H. Kiesewalter, M. Martin, C.-Y. Hsu, R. Hartmann, T. Wechsler, C. Eriksen, S. Brix, K. Drescher, N.R. Stanley-Wall, R. Kümmerli, A.T. Kovacs, Division of labor during biofilm matrix production, Curr. Biol. 28 (2018) 1903–1913.
[6] W.K. Smits, O.P. Kuipers, J.-W. Veening, Phenotypic variation in bacteria: the role of feedback regulation, Nat. Rev. Microbiol. 4 (2006) 259–271.
[7] J.W. Costerton, Z. Lewandowski, D.E. Caldwell, D.R. Korber, H.M. Lappin-Scott, Microbial biofilms, Annu. Rev. Microbiol. 49 (1995) 711–745.
[8] L. Hall-Stoodley, J.W. Costerton, P. Stoodley, Bacterial biofilms: from the natural environment to infectious diseases, Nat. Rev. Microbiol. 2 (2004) 95–108.
[9] H.-C. Flemming, J. Wingender, The biofilm matrix, Nat. Rev. Microbiol. 8 (2010) 623–633.
[10] G.G. Anderson, G.A. O'Toole, Innate and induced resistance mechanisms of bacterial biofilms, Curr. Top. Microbiol. Immunol. 322 (2008) 87–107.
[11] K. Lewis, Multidrug tolerance of biofilms and persister cells, Curr. Top. Microbiol. Immunol. 322 (2008) 107–131.
[12] D.O. Serra, A.M. Richter, R. Hengge, Cellulose as an architectural element in spatially structured *Escherichia coli* biofilms, J. Bacteriol. 195 (2013) 5540–5554.
[13] C. Aguilar, H. Vlamakis, R. Losick, R. Kolter, Thinking about *Bacillus subtilis* as a multicellular organism, Curr. Opin. Microbiol. 10 (2007) 638–643.
[14] H. Vlamakis, Y. Chai, P. Beauregard, R. Losick, R. Kolter, Sticking together: building a biofilm the *Bacillus subtilis* way, Nat. Rev. Microbiol. 11 (2013) 157–168.
[15] D.O. Serra, A.M. Richter, G. Klauck, F. Mika, R. Hengge, Microanatomy at cellular resolution and spatial order of physiological differentiation in a bacterial biofilm, mBio 4 (2) (2013) e00103–e00113.
[16] W. Thongsomboon, D.O. Serra, A. Possling, C. Hadjineophytou, R. Hengge, L. Cegelski, Phosphoethanolamine cellulose: a naturally produced chemically modified cellulose, Science 359 (2018) 334–338.
[17] Y. Chai, F. Chu, R. Kolter, R. Losick, Bistability and biofilm formation in *Bacillus subtilis*, Mol. Microbiol. 67 (2008) 254–263.
[18] H. Vlamakis, C. Aguilar, R. Losick, R. Kolter, Control of cell fate by the formation of an architecturally complex bacterial community, Genes Dev. 22 (2008) 945–953.
[19] D.O. Serra, R. Hengge, Stress responses go three-dimensional—the spatial order of physiological differentiation in bacterial macrocolony biofilms, Environ. Microbiol. 16 (2014) 1455–1471.
[20] G. Klauck, D.O. Serra, A. Possling, R. Hengge, Spatial organization of different sigma factor activities and c-di-GMP signalling within the three-dimensional landscape of a bacterial biofilm, Open Biol. 8 (2018), 180066.
[21] P.S. Stewart, M.J. Franklin, Physiological heterogeneity in biofilms, Nat. Rev. Microbiol. 6 (2008) 199–210.
[22] H. Weber, C. Pesavento, A. Possling, G. Tischendorf, R. Hengge, Cyclic-di-GMP-mediated signaling within the σ^S network of *Escherichia coli*, Mol. Microbiol. 62 (2006) 1014–1034.
[23] C. Pesavento, G. Becker, N. Sommerfeldt, A. Possling, N. Tschowri, A. Mehlis, R. Hengge, Inverse regulatory coordination of motility and curli-mediated adhesion in *Escherichia coli*, Genes Dev. 22 (2008) 2434–2446.
[24] S. Lindenberg, G. Klauck, C. Pesavento, E. Klauck, R. Hengge, The EAL domain phosphodiesterase YciR acts as a trigger enzyme in a c-di-GMP signaling cascade in *E. coli* biofilm control, EMBO J. 32 (2013) 2001–2014.
[25] R. Hengge, Principles of cyclic-di-GMP signaling, Nat. Rev. Microbiol. 7 (2009) 263–273.
[26] R. Hengge, Role of c-di-GMP in the regulatory networks of *Escherichia coli*, in: A.J. Wolfe, K.L. Visick (Eds.), The

Second Messenger Cyclic-di-GMP, ASM Press, Washington, D.C. 2010, pp. 230–252.
[27] R. Hengge, Trigger phosphodiesterases as a novel class of c-di-GMP effector proteins, Philos. Trans. R. Soc. B 371 (2016), 20150498.
[28] K.P. Yousef, A. Streck, C. Schütte, H. Siebert, R. Hengge, M. von Kleist, Logical-continuous modelling of post-translationally regulated bistability of curli fiber expression in *Escherichia coli*, BMC Bioinf. 9 (2015) 39.
[29] C. Barembruch, R. Hengge, Cellular levels and activity of the flagellar sigma factor FliA of *Escherichia coli* are controlled by FlgM-modulated proteolysis, Mol. Microbiol. 65 (2007) 76–89.
[30] F. Mika, S. Busse, A. Possling, J. Berkholz, N. Tschowri, N. Sommerfeldt, M. Pruteanu, R. Hengge, Targeting of *csgD* by the small regulatory RNA RprA links stationary phase, biofilm formation and cell envelope stress in *Escherichia coli*, Mol. Microbiol. 84 (2012) 51–65.
[31] N. Sommerfeldt, A. Possling, G. Becker, C. Pesavento, N. Tschowri, R. Hengge, Gene expression patterns and differential input into curli fimbriae regulation of all GGDEF/EAL domain proteins in *Escherichia coli*, Microbiology 155 (2009) 1318–1331.
[32] P.K. Brown, C.M. Dozois, C.A. Nickerson, A. Zuppardo, J. Terlonge, R. Curtiss III, MlrA, a novel regulator of curli (Agf) and extracellular matrix synthesis by *Escherichia coli* and *Salmonella enterica* serovar typhimurium, Mol. Microbiol. 41 (2001) 349–363.
[33] O. Sarenko, G. Klauck, F.M. Wilke, V. Pfiffer, A.M. Richter, S. Herbst, V. Kaever, R. Hengge, More than enzymes that make and break c-di-GMP—the protein interaction network of GGDEF/EAL domain proteins of *Escherichia coli*, mBio 8 (2017) e01639-17.
[34] N. Grantcharova, V. Peters, C. Monteiro, K. Zakikhany, U. Römling, Bistable expression of CsgD in biofilm development of *Salmonella enterica* serovar typhimurium, J. Bacteriol. 192 (2010) 456–466.
[35] K.D. MacKenzie, Y. Wang, D.J. Shivak, C.S. Wong, L.J. Hoffman, S. Lam, C. Kröger, A.D. Cameron, H.G. Townsend, W. Köster, A.P. White, Bistable expression of CsgD in *Salmonella enterica* serovar Typhimurium connects virulence to persistence, Infect. Immun. 83 (2015) 2312–2326.
[36] M.B. Elowitz, S. Leibler, A synthetic oscillatory network of transcriptional regulators, Nature 403 (2000) 335–338.
[37] W. Xiong, E. Ferrell Jr., A positive-feedback-based bistable "memory module" that governs a cell fate decision, Nature 426 (2003) 460–465.
[38] U. Alon, An Introduction to Systems Biology: Design Principles of Biological Circuits, Chapman & Hall/CRC, London, UK, 2007.
[39] F.M. Commichau, J. Stülke, Trigger enzymes: bifunctional proteins active in metabolism and controlling gene expression, Mol. Microbiol. 67 (2008) 692–702.
[40] A. Boehm, M. Kaiser, H. Li, C. Spangler, C.A., K, M. Ackerman, V. Kaever, V. Sourjik, V. Roth, U. Jenal, Second messenger-mediated adjustment of bacterial swimming velocity, Cell 141 (2010) 107–116.
[41] X. Fang, M. Gomelsky, A post-translational, c-di-GMP-dependent mechanism regulating flagellar motility, Mol. Microbiol. 76 (2010) 1295–1305.
[42] K. Paul, V. Nieto, W.C. Carlquist, D.F. Blair, R.M. Harshey, The c-di-GMP binding protein YcgR controls flagellar motor direction and speed to affect chemotaxis by a "backstop brake" mechanism, Mol. Cell 38 (2010) 128–139.
[43] H.S. Girgis, Y. Liu, W.S. Ryu, S. Tavazoie, A comprehensive genetic characterization of bacterial motility, PLoS Genet. 3 (2007) e154.
[44] K. Hayashi, N. Morooka, Y. Yamamoto, K. Fujita, K. Isono, S. Choi, E. Ohtsubo, T. Baba, B.L. Wanner, H. Mori, T. Horiuchi, Highly accurate genome sequences of *Escherichia coli* K-12 strains MG1655 and W3110, Mol. Syst. Biol. 2 (2006) (2006) 0007.
[45] K.A. Datsenko, B.L. Wanner, One-step inactivation of chromosomal genes in *Escherichia coli* K-12 using PCR products, Proc. Natl. Acad. Sci. U. S. A. 97 (2000) 6640–6645.
[46] J.H. Miller, Experiments in Molecular Genetics, Cold Spring Harbor Laboratory, Cold Spring Harbor, N. Y, 1972.
[47] D.O. Serra, R. Hengge, Experimental detection and visualization of the extracellular matrix in macrocolony biofilms, in: K. Sauer (Ed.), C-di-GMP Signaling: Methods & Protocols—Methods in Molecular Biology, Humana Press, Springer Nature, New York, N.Y 2017, pp. 133–145.
[48] W. Bokranz, X. Wang, H. Tschape, U. Römling, Expression of cellulose and curli fimbriae by *Escherichia coli* isolated from the gastrointestinal tract, J. Med. Microbiol. 54 (2005) 1171–1182.